SAND2008-6021C

Computational Fluid Dynamics Modeling of UV Reactor Validation Tests

Edward Wicklein and Harold Wright
Carollo Engineers, Seattle, WA, ewicklein@carollo.com

Clifford K. Ho
Sandia National Laboratories, Albuquerque, NM

ABSTRACT

Computational fluid dynamics modeling (CFD) is a tool that has been shown to successfully determine relative differences in ultraviolet (UV) reactor performance. This paper presents a comparison of CFD modeling coupled with a UV intensity model to reproduce validation tests for several UV reactors. The study demonstrated that a hydraulic grid independent solution could be achieved. At lower UVT the modeling approach predicts the dose fairly well; however, there is deviation in the results at higher UVT.

Introduction

Ultraviolet (UV) disinfection is being increasingly used for drinking water treatment. The UV dose delivered to a flow is dependent on the hydraulics through the reactor, which is a function of the piping system the reactor is installed in, coupled with the UV reactor geometry. UV reactors undergo validation testing to determine the relations between delivered dose and flowrate, water UV transmittance (UVT) and lamp output. To provide conservative estimates of dose delivery, testing is typically conducted using inlet and output piping to the reactor that will produce challenging hydraulics and therefore a conservative dose. However, the installation in the field may be quite different from the initial validation arrangement requiring further validation testing. Because the testing can be costly and difficult to conduct, engineers and scientists desire better tools to evaluate how a system will work during the design phase when changes are less expensive to make. In addition, predictive tools and models can help to facilitate installation of UV reactor systems at sites where the inlet and outlet piping may be different than the validated configuration.

Several UV reactor validation tests were simulated using numerical modeling techniques. The flow field was calculated with a commercial 3-dimensional (3D) computational fluid dynamics model, and the dose was calculated with UVXPT, a software package under development by Carollo Engineers to model UV intensity fields, UV sensor readings, UV dose delivery, and microbial inactivation (Wright and Reddy 2003). UVXPT uses Microsoft Excel as a user interface. The software is programmed in Visual Basic and is accessed using command buttons.

Model Development Overview

The computational meshes for all reactors discussed in this paper and a companion paper (Ho. et al. 2008, this proceedings) were developed using the same procedure with the grid generation software, GAMBIT (v. 2.4.6), developed for FLUENT. The details of Gambit and Fluent can be found in the respective User's Guides (Fluent 2006, Fluent 2007). The 3D geometry of the main portions of the flow domain were developed using points, lines, surfaces and volumes based on drawings included in the validation reports, as well as additional shop drawings supplied by the respective UV manufacturer. The upstream and downstream piping configuration used during validation testing that may have impacted the hydraulics within the reactor was included in the overall domain. The key internal wetted details within the respective

reactor were included in the domain, including the lamp sleeves, the wiper drive screw, the sensor bodies, and baffles, if appropriate.

The 3D geometry was used as a base to define the computational grid, using a similar procedure for all of the reactors modeled. In all cases a hybrid mesh was used for modeling the reactors, primarily comprised of hexahedral elements. A hexahedral Cooper scheme was used for the inlet an outlet piping, with defined boundary layer cells at the walls. The reactors were meshed with a tet/hybrid scheme using a hexahedral core mesh, with tetrahedral, pyramid, and prism elements transitioning from the core region to the walls. The boundary faces were defined and the grid exported for use in the solver, FLUENT (v. 6.3.26). Due to the complexity of the intersecting curved surfaces within the reactor, maintaining high quality elements was not always possible. However, for all cases the worst quality tetrahedral elements had skew ratio of 0.83. Therefore, once the grid was read into FLUENT, the polyhedral conversion tool was used to improve the mesh quality by further reducing the number of skewed cells.

In all cases, an inflow velocity was applied at the upstream end of the model using a uniform velocity distribution corresponding to the respective test conditions flow rate. All of the validation tests included between 1 and 3 elbows upstream from the reactor. Some of the validation tests also included expansions or contractions in the piping. The upstream boundary was set 5 pipe diameters upstream from the most upstream fitting if there were 3 or more fittings upstream from the reactor, and 10 diameters if there were only one or two fittings. The upstream piping created a fully develop flow condition entering the reactor, free from boundary influence. The downstream boundary was an outflow boundary, approximately 5 diameters downstream from the reactor exit fitting, typically a contraction or expansion. All other surfaces were wall boundaries. The κ-ε realizable turbulence model was used in all cases, with the standard wall function. The models were all run to steady state in double precision. The solution was calculated with the SIMPLE algorithm utilizing a second order accurate dicretization. The hydraulic models were run to a converged solution, defined by an absolute residual of less than 0.001 for all solved variables.

Following initial grid development, a grid sensitivity analysis was carried out to verify that the hydraulic and UV-dose solutions were grid independent. For each sensitivity run, the velocity magnitude at 100 discrete points distributed before and after the reactor were compared between model runs on different grids. The data were plotted to determine a correlation coefficient for the pairs of grid comparison (medium vs. initial, fine vs. medium). For correlation coefficients close to 1, the simulated velocities were similar between the two grids.

Additional grid comparisons were made for the delivered UV dose. The UVXPT software package was used to model UV intensity fields, UV sensor readings, UV dose delivery, and microbial inactivation. For the UVXPT runs discussed in this paper, approximately 2000 particles were released upstream of the reactor, close the model inlet, and tracked in time as they traveled through the system.

Calgon 12" Sentinel® Reactor Model

The complete model domain of the Calgon Sentinel® reactor as validated is shown in Figure 1. The model began with a 12-inch diameter straight pipe section approximately 10 pipe diameters long. The straight piping was followed by a single 90-degree elbow approximately 4 pipe diameters upstream from the reactor. The reactor included the outer surface of the lamp sleeves, the sensor bodies, and included both horizontal and vertical baffles to direct flow

toward the lamps. A second 90-degree elbow was located approximately 1 diameter downstream from the reactor, followed by a concentric expansion to 18-in diameter pipe.

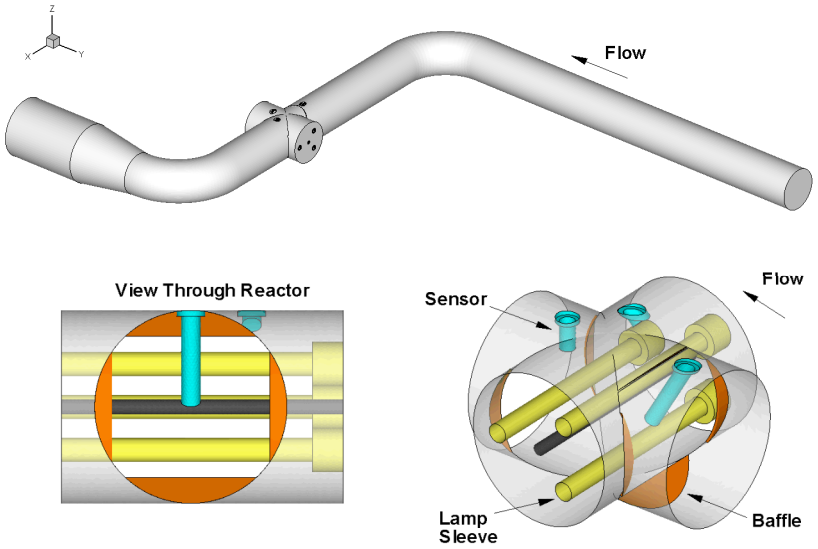

Figure 1. GAMBIT/FLUENT model of the Calgon Sentinel® reactor and piping.

A grid sensitivity analysis was performed on the reactor grid by reducing the reactor cell size, increasing the total cell count of the reactor for two iterations from the initial grid, while maintaining a constant piping cell size with a range of 0.25-inches to 2 inches. The reactor was meshed using a tetrahedral/hybrid mesh with a hexahedral core. Table 1 summarizes the model cell count and results of the velocity magnitude comparison for the three model grids evaluated, and Figure 2 graphically shows the comparison. In all sensitivity cases the model was run at a flow of 4.9 mgd. The velocity comparison was made at points located at the exit of the reactor, and the correlation coefficient is presented for the pairs of grid comparisons (medium vs. initial, fine vs. medium).

Table 1. Summary of grid independence study for Calgon 12" Sentinel® reactor.

Grid	No. of Cells in Reactor	Percent Increase in Number of Cells	No. of Cells in Piping	Total Cells	Velocity Magnitude Correlation R^2
Initial	465,652	---	249,500	715,152	---
Medium	610,716	31	249,500	860,216	0.85
Fine	753,564	23	249,500	1,003,064	0.98

Data comparisons showed that the initial and medium grid only had a correlation coefficient of 0.85, whereas the medium and fine grids had a correction of 0.98. Therefore, the medium or fine grid produces a grid independent solution. The core element size in the medium grid reactor was 0.23-inches, with surface elements as small as 0.12-inches. The reactor grid contains 610,716 elements for total model size of 860,216 elements. Figure 3 shows a section of the grid through the piping, as well as the fine grid on the outer surfaces of the reactor.

The simulated velocity profile in the Calgon Sentinel® reactor at 4.9 mgd is shown in Figure 4. The figure shows both a vertical and horizontal section through the reactor centerline. The velocity in the 12-inch diameter piping approaching the reactor is 2.7 m/s. The baffles at the entrance to the reactor constrict the flow area increasing the velocity and directing flow toward the lamps. Flow accelerates around the upstream lamps, reaching a velocity of 5.5 m/s above and below the upstream lamps. The velocity is very low in the wake region behind the baffles. The peak velocity around the downstream lamp is approximately 4.5 m/s. In plan view, the wake region behind the leading sensor appears to extend past the downstream lamp.

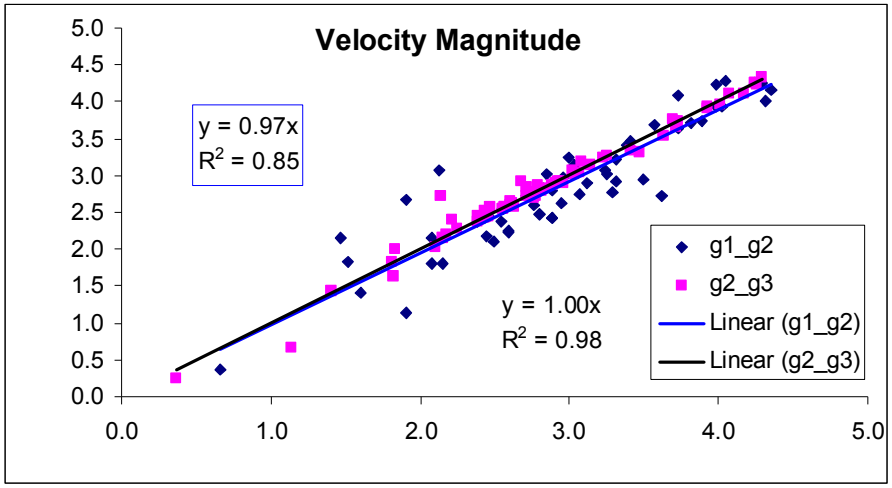

Figure 2. Comparison of velocity magnitude for the three Calgon Sentinel® grids modeled.

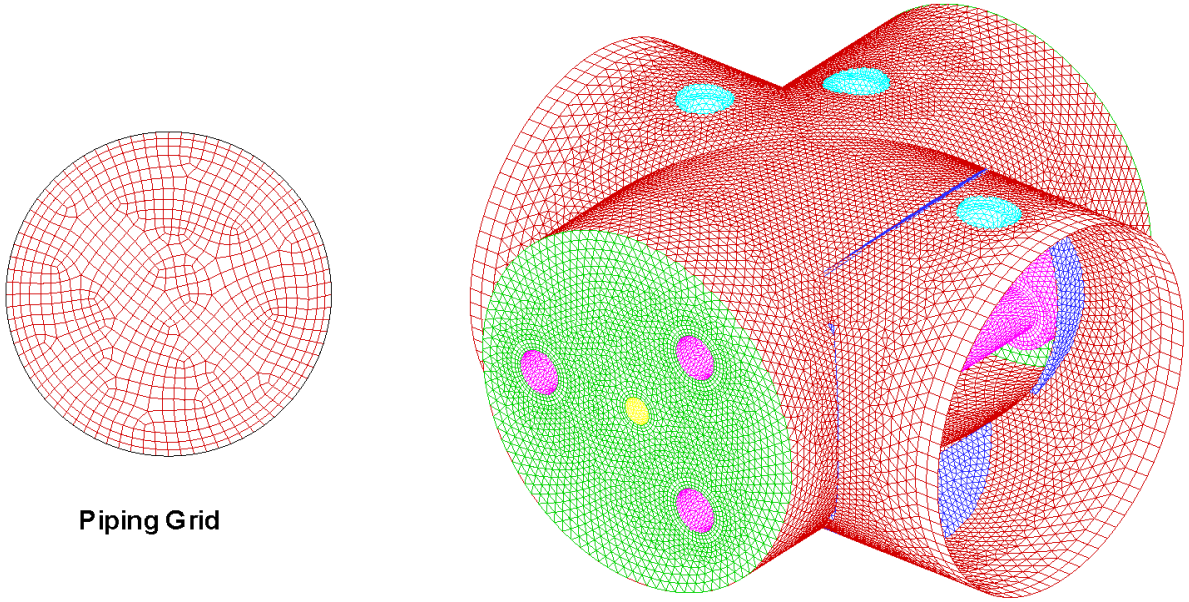

Figure 3. Section of piping grid, and fine model grid on surfaces of the Calgon Sentinel® Reactor

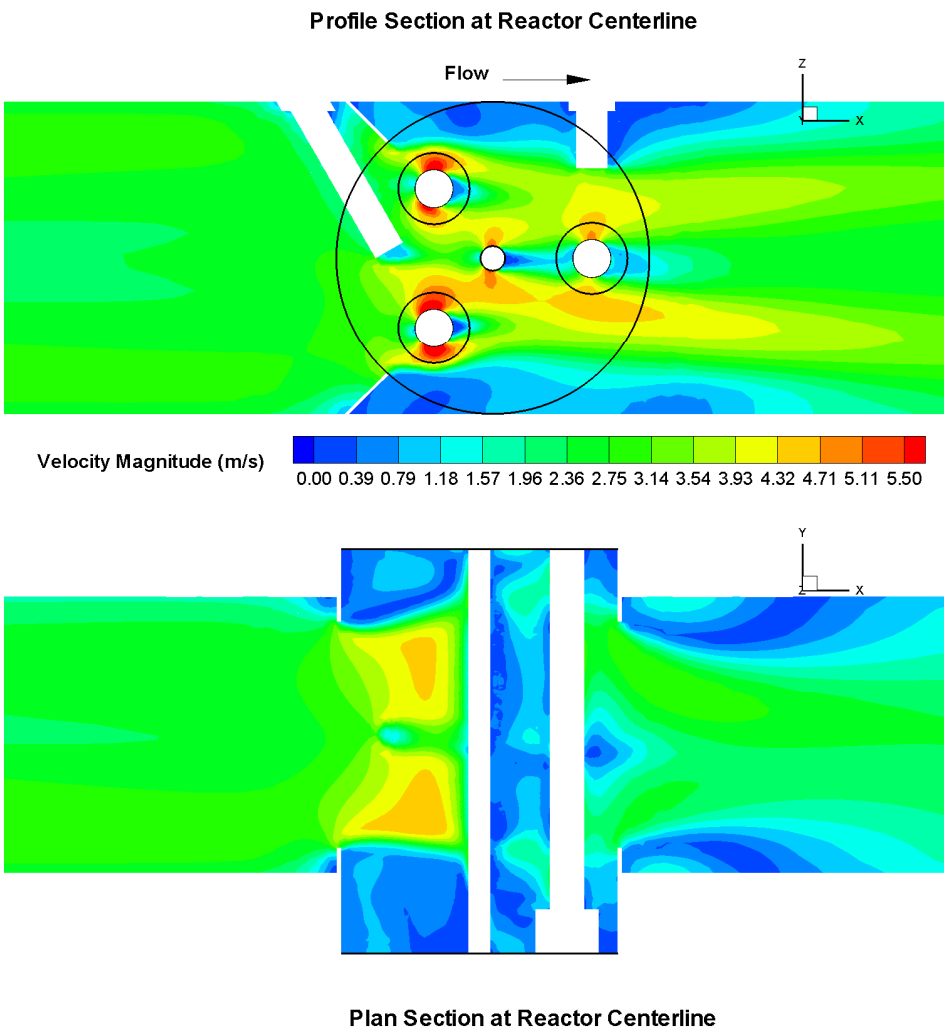

Figure 4. Simulated velocity profiles along cutplanes through the center of the Calgon Sentinel® reactor. Top: side view. Bottom: plan view.

The UVXPT model was applied using the initial mesh and particle tracks. The UV output of the MP lamp used in the UVXPT simulation was calibrated by comparing predicted UV sensor readings to UV sensor readings measured during UV validation testing. All of the particle tracks made their way through the reactor. For rapid analysis, UVXPT scaled the time steps of the particle tracks obtained with the 4.9 mgd Fluent simulation to simulate particle tracks expected at other flow rates. Figure 5 shows examples of the predicted dose distribution with the Calgon reactor. Test conditions for each image in Figure 5 are as follows:

- Top left: UVT = 69.8%, flow = 0.59 mgd, lamp output = 55.55 %, and one lamp on.
- Top right: UVT = 98.3%, flow = 4.81 mgd, lamp output = 84.44 %, and one lamp on.
- Bottom left: UVT = 69.9%, flow = 0.30 mgd, lamp output ~ 26 %, and three lamps on.
- Bottom right: UVT = 98.6%, flow = 2.40 mgd, lamp output ~ 32 %, and three lamps on.

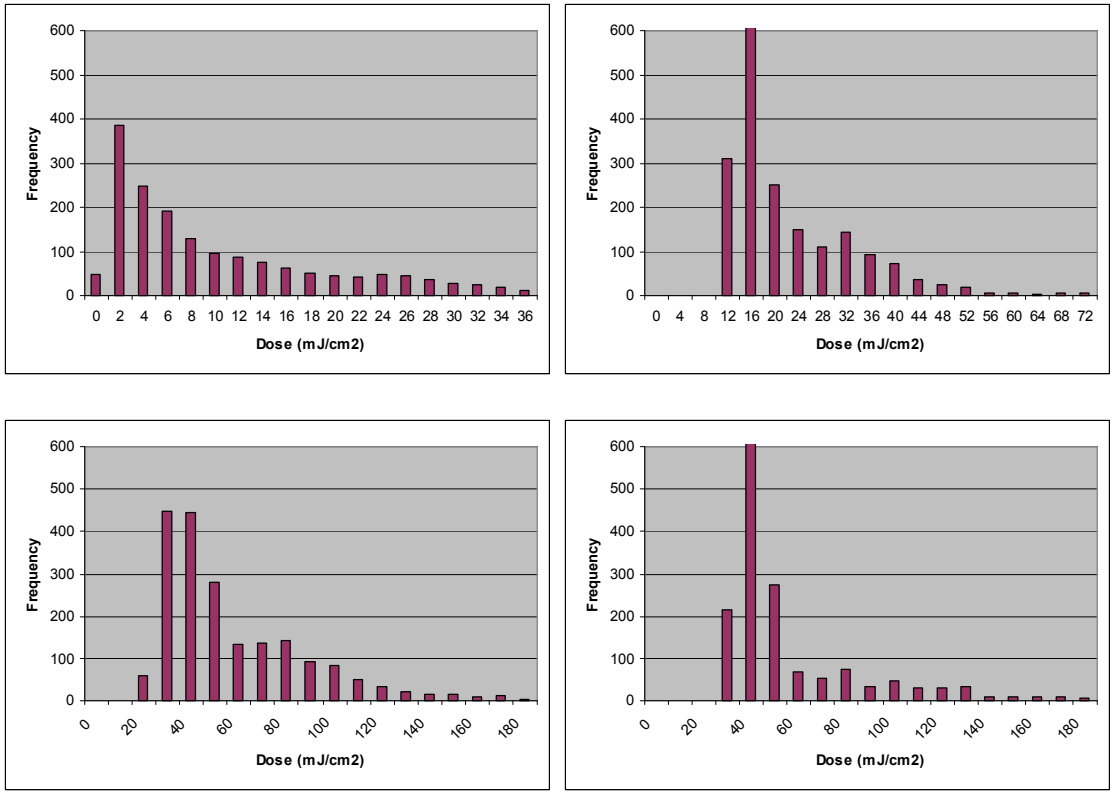

Figure 5. UV dose distributions for the Calgon Sentinel® reactor.

The Calgon reactor was validated at the Portland UV Validation test Facility using MS2 phage as a test microbe. Figure 6 shows a plot of measured versus predicted MS2 RED. The following observations are made from the data:

- For a given UVT, the relation between measured and predicted RED is fitted with the relation y=Ax with an R-squared ranging from 0.9778 to 0.9926 and average 0.9829. The high R-squared shows that the model is accounting for the impacts of flowrate (0.3 to 4.9 mgd), lamp on/off status, and relative lamp output reasonably well.

- At low UVTs from 70 to 88 %, the slope of the relation between measured and predicted RED for a given UVT ranges from 0.9569 to 0.9806 and averages 0.9674. This observation suggests that the CFD-model is providing good predictions of dose delivery by the reactor at those UVTs. An important observation is that these results were obtained without any “CFD calibration factor”. If the model provides accurate predictions without application of a CFD factor, then it is accounting for the hydraulics through the reactor caused by the upstream and downstream piping (which include a ninety degree bend upstream) and baffle plates and lamps within the reactor. This implies that the model would provide valid predictions if the simulated inlet piping were changed.

- At high UVTs above 88%, the slope of the relation between measured and predicted RED for a given UVT increases with UVT. The slope is 1.05 at 94% UVT and 1.21 at 98% UVT. We suspect that the increased slope occurs because the UVXPT model is not incorporating wall reflections. Future work will incorporate reflections within the UVXPT

algorithm. Ho et al. (2008, these proceedings) provides additional analyses of wall reflection.

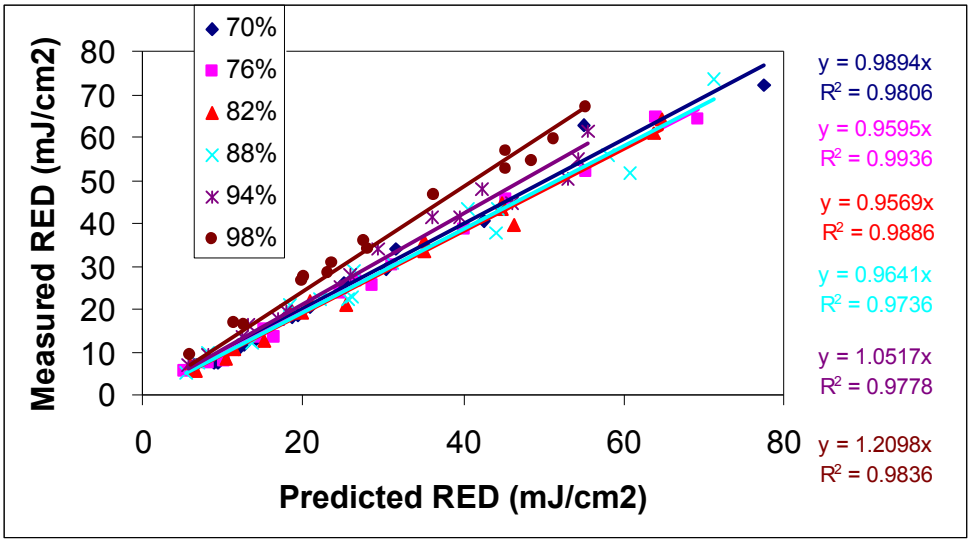

Figure 6. Measured versus predicted MS2 RED for the Calgon Sentinel® reactor.

The observation that the CFD model obtained for a flowrate of 4.9 mgd provides good predictions at flow rates from 0.3 to 4.9 mgd implies that the scaling of the time step used by UVXPT is a reasonable approach.

Degremont Technologies Ozonia Aquaray® H_20 20" Reactor Models

The Ozonia Aquaray® H_2O 20" reactor was validated at the DVGW test facility in two configurations, the M-rig, which utilized a single reactor installed in 12-inch piping, and the L-rig, which utilized two reactors in series installed in 24-inch piping. Models were developed for both configurations and evaluated.

The M-rig model, shown in Figure 7, began with a section of straight 12-inch diameter pipe 60-inches long (5 pipe diameters), leading to a 90-degree elbow. The piping then ran straight to a S-bend, which included two 90-degree elbows separated by a short spool section. The S-bend was followed by a concentric expansion, which connected to the reactor. The reactor included 6 lamp sleeves, the wiper power screw, the outside surfaces of the sensors, and baffles. A concentric reducer is located downstream from the reactor, followed by approximately 5 diameters of 12-inch diameter straight piping. For some test conditions with the M-rig, a porous baffle plate was located within the piping between the concentric expansion and the reactor.

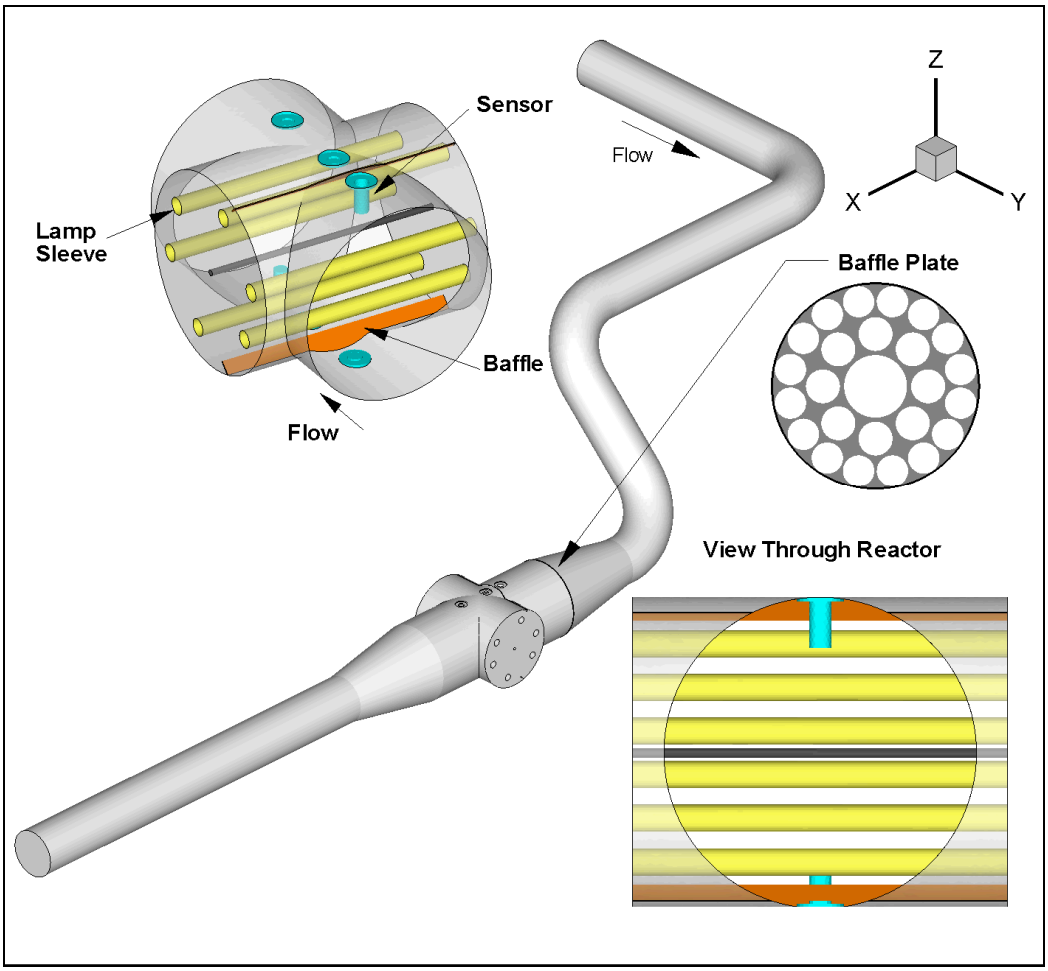

Figure 7. M-rig GAMBIT/FLUENT model of the Ozonia Aquaray® H_2O 20" reactor and piping.

The L-rig model, shown in Figure 8, began with a section of straight 24-inch diameter pipe 120-inches (5 pipe diameters), leading to a S-bend, which included two 90-degree elbows, separated by a short spool section. The S-bend was followed by a concentric reducer, which was attached to the upstream reactor. A second reactor was attached to the downstream end of the first reactor and followed by a concentric expansion back to 24-inch diameter pipe, which ran straight for approximately 5 diameters to the model outlet.

For both the M-rig and L-rig model runs, a similar procedure was used to generate the model grids. The piping was primarily meshed with hexahedral elements using a Cooper scheme, and includes boundary layer elements at the surface. The M-rig had 1,120 cells in a piping cross section, and the L-rig utilized 1,092 cells at a given pipe cross section. The piping elements were held constant with a minimum cell dimension of 0.4 inches for the M-rig, and 0.8 inches for the L-Rig for each case.

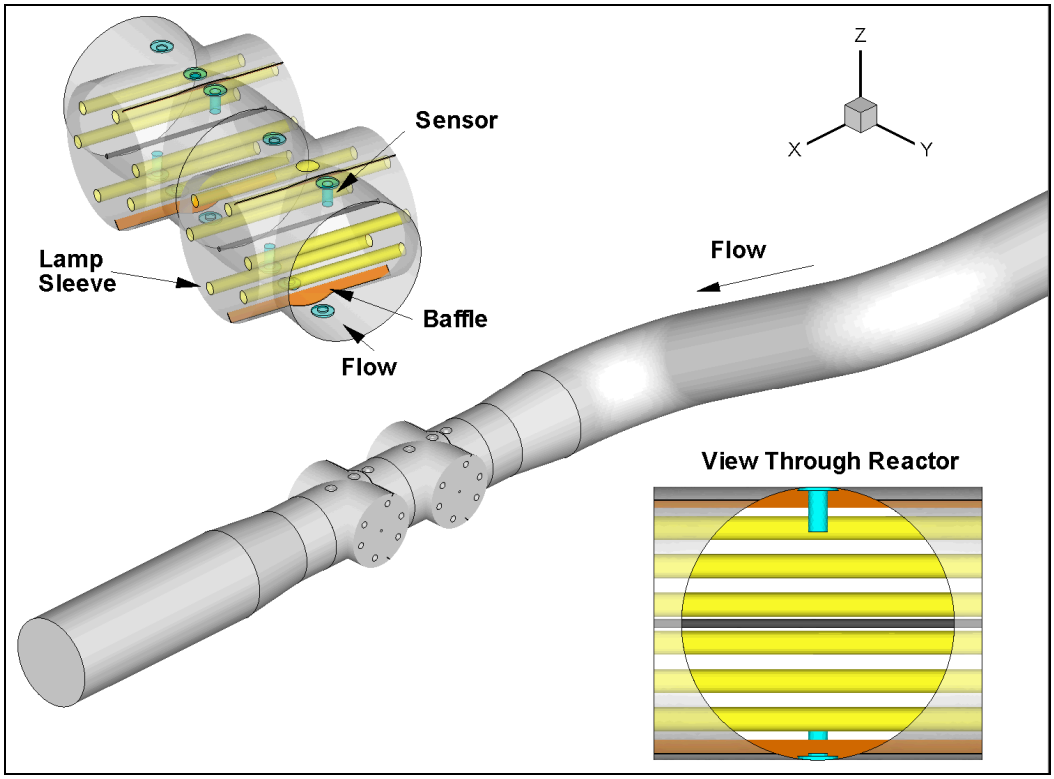

Figure 8. L-rig GAMBIT/FLUENT model of the Ozonia Aquaray® H_2O 20" reactor and piping.

As with the Calgon Sentinel® model, a grid sensitivity analysis was performed by progressively reducing the cell size within the reactor, while holding the piping size constant. Interface boundaries were used to transition the coarser piping grid to the finer reactor grid. The grid refinement runs were carried out for both the M-rig and L-rig configurations. The M-rig and L-rig utilized the same reactor grid, with the exception of the interface between the two reactors in the L-rig where the grid was slightly altered to match one- to-one. The reactor was meshed using a Cooper scheme through the center along the lamp axis, and a tetrahedral/hybrid mesh with a hexahedral core was used to transition to the outer walls. The minimum tetrahedral cell quality was 0.82. The overall number of skewed cells was further using the polyhedral conversion tool within Fluent. The M-rig grids with and without the baffle were identical, except that the cells representing the solid baffle area were changed from solid to fluid when the baffle was not present. The M-rig was evaluated at a flow rate of 4.44 mgd, and the L-rig was evaluated at a flow rate of 7.61 mgd.

Table 2 summarizes the size of the model grids evaluated, the percent refinement, as well as the velocity magnitude correlation for the pairs of grid comparison (medium vs. initial, fine vs. medium). Figure 9 shows a plot of the comparison for the M-rig runs without the baffle. Figure 10 presents a plot of the data comparison for the M-rig with the baffle. Figure 11 presents the comparison for the L-rig runs. For all runs the velocity comparison improved, or matched very closely for the progressively refined grids.

Additional runs were made with the L-rig at a high flow condition of 19.97 mgd and at a low flow condition of 4.82 mgd to evaluate the reactor head loss. Figure 12 shows a comparison

between the measured head loss and the calculated head loss. The CFD model calculates the head loss for low and mid flows very well, while there is a slight variation at the high flow case.

Figure 13 shows the model grid at a section through the piping, and at surface of the reactor. Figures 14 and Figure 15 show a comparisons of the velocity magnitude at the reactor centerline in plan and profile for the M-rig with and without baffle at 700 m^3/h. In section view, the velocity is higher at the bottom of the reactor and toward the right side looking downstream for the run without the baffle. With the baffle installed, the velocity is better distributed approaching the lamps. Figure 16 show the velocity magnitude at the reactor centerlines in plan and profile in the L-rig configuration. The velocity is fairly uniform approaching the first reactor, and the velocity distribution is similar for both reactors.

Table 2. Summary of grid independence study for Ozonia Aquaray® H_2O 20" reactor.

Configuration	Grid	No. of Cells in Reactor	Percent Increase in Number of Cells	No. of Cells in Piping	Total Cells	Velocity Magnitude Correlation R^2
M-rig no baffle	Initial (G0)	494,989	---	669,706	1,164,695	---
	Medium (G1)	681,734	38	682,306	1,364,040	0.93
	Fine (G2)	898,296	32	672,706	1,571,002	0.99
M-rig with baffle	Initial (G0)	494,989	---	668,959	1,163,948	---
	Medium (G1)	681,734	38	681,559	1,363,293	0.96
	Fine (G2)	898,296	32	671,959	1,570,255	0.99
L-rig	Initial (G0)	971,546	---	555,828	1,527,374	---
	Medium (G1)	1,351,067	39	555,828	1,906,895	0.99
	Fine (G2)	1,785,296	32	555,828	2,341,124	0.99

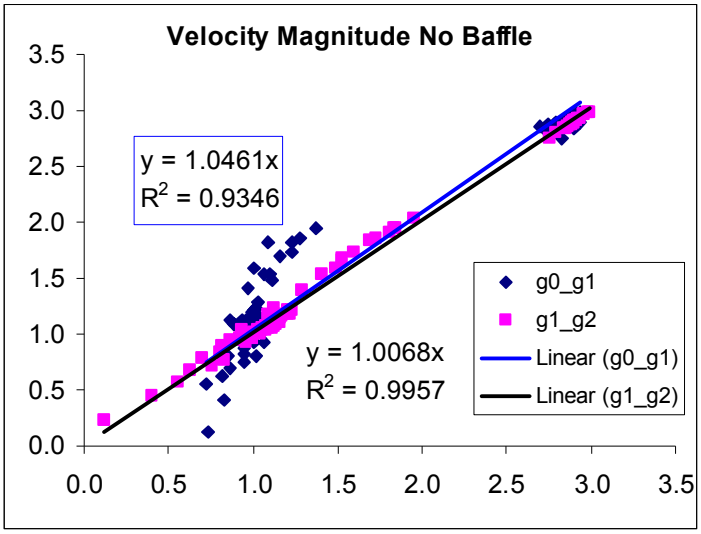

Figure 9. Point data comparison between grids for M-rig runs without the baffle.

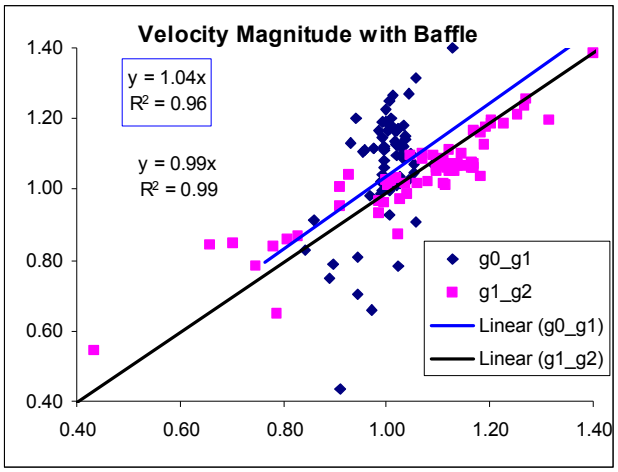

Figure 10. Point data comparison between grids for M-rig runs with the baffle.

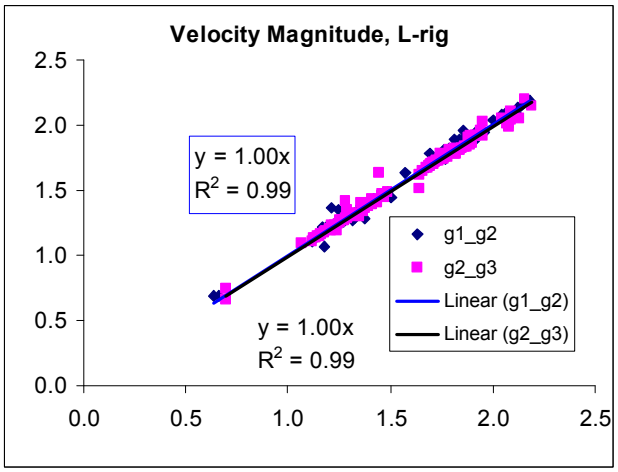

Figure 11. Point data comparison between grids for the L-rig runs.

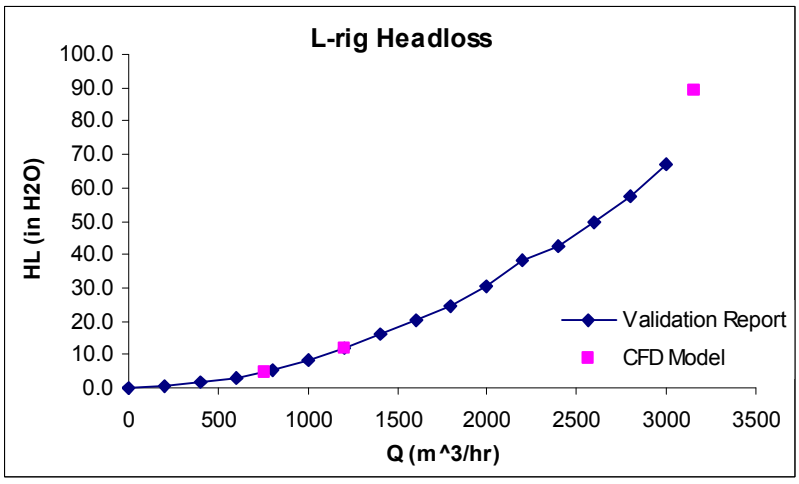

Figure12. Comparison of measured and modeled head loss for the L-rig configuration.

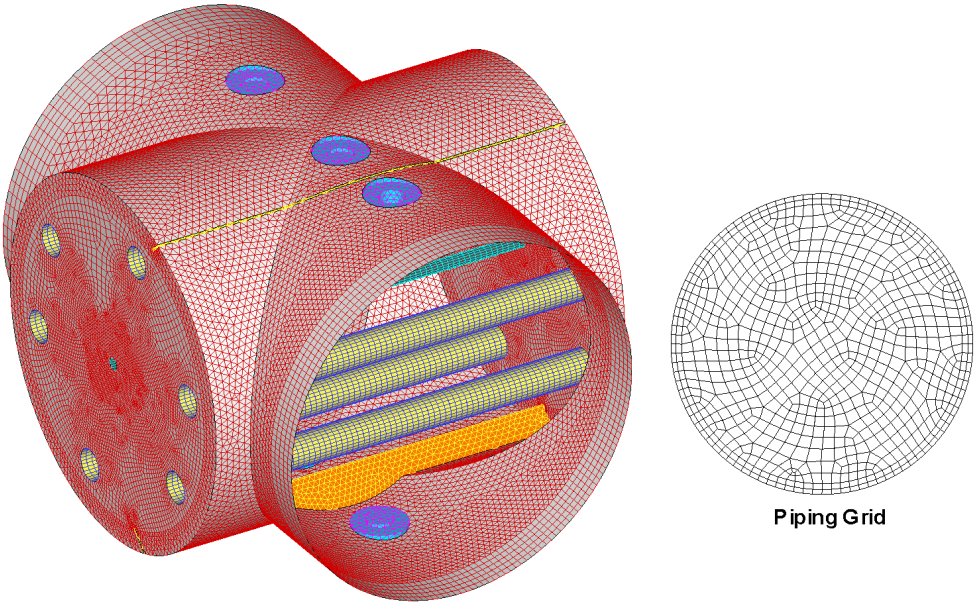

Figure 13. Grid at IDI Aquaray surface and at section in piping.

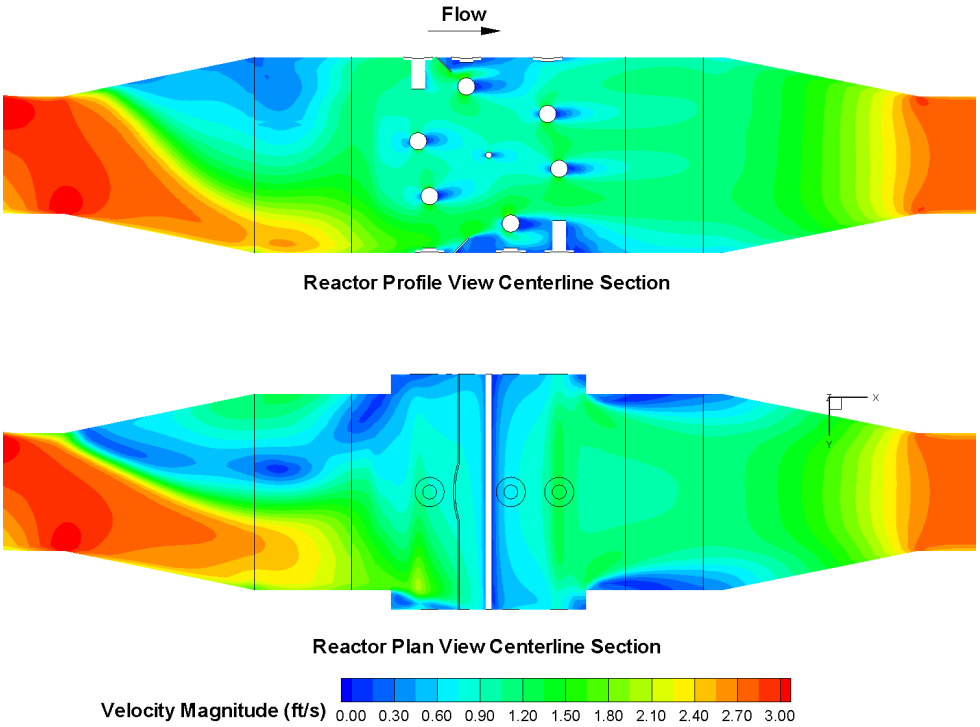

Figure 14. Velocity magnitude at reactor centerline sections in plan and profile for M-rig without baffle at 4.44 mgd

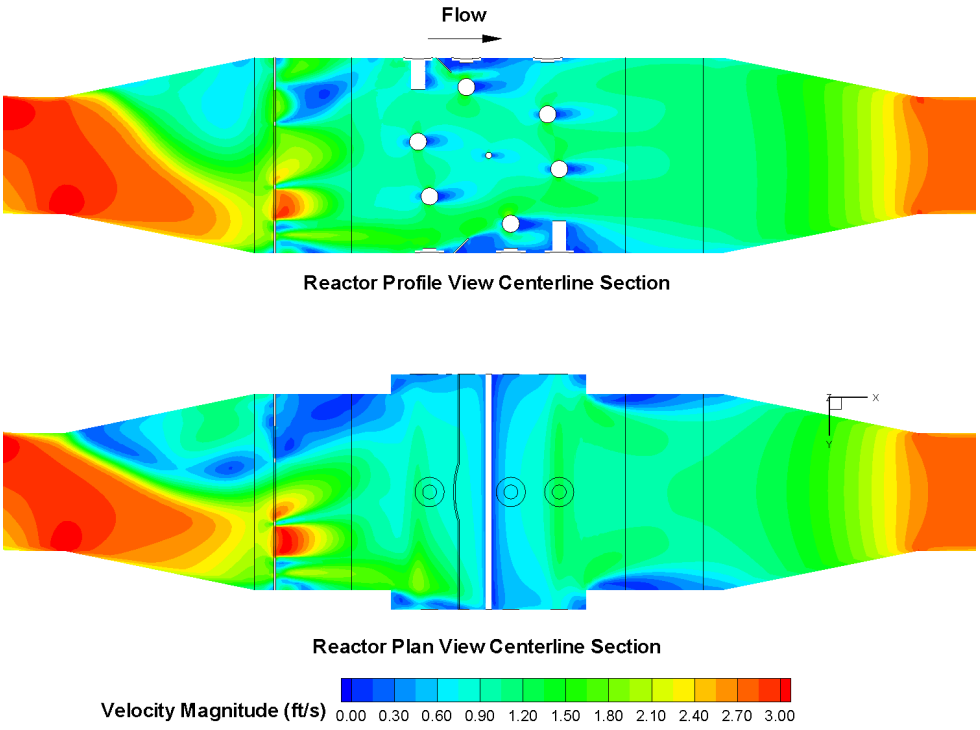

Figure 15. Velocity magnitude at reactor centerline sections in plan and profile for M-rig with baffle at 4.44 mgd

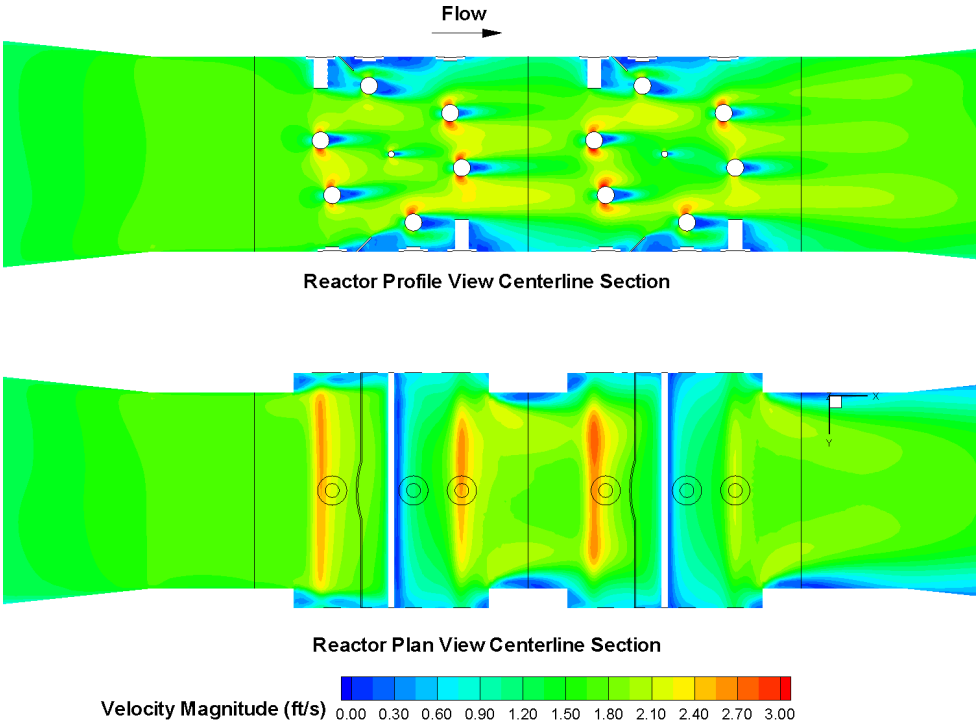

Figure 16. Velocity magnitude at reactor centerline sections in plan and profile for the L-rig with baffle at 7.61 mgd

Predictions of RED for M-Rig and L-Rig Reactors using UVXPT

Particle tracks for the Ozonia Aquaray® H_2O 20" reactors were developed from the CFD models for the three validation configurations. Particle tracks with the M-rig were predicted using a CFD flowrate of 4.44 mgd while particle tracks for the L-rig were predicted at a CFD flowrate of 7.61 mgd. With each reactor configuration, particle tracks were developed for three grid mesh densities, identified as initial (G0), medium (G1) and fine (G2).

Figure 17 compares the measured B. subtilis RED with the M-rig without baffle plate to the RED predicted using the G1 mesh. The data shows an excellent correlation between measured and predicted RED at low UVTs of 92%. At 98% UVT, the relation between measured and predicted RED was fitted using a linear relation with a notable intercept and with a much lower R-squared. Based on data observed with the Calgon reactor, wall reflections may have an impact on the measured RED; the predicted REDs reported here do not account for reflections. Ho et al. (2008, these proceedings) provides additional analyses of wall reflection.

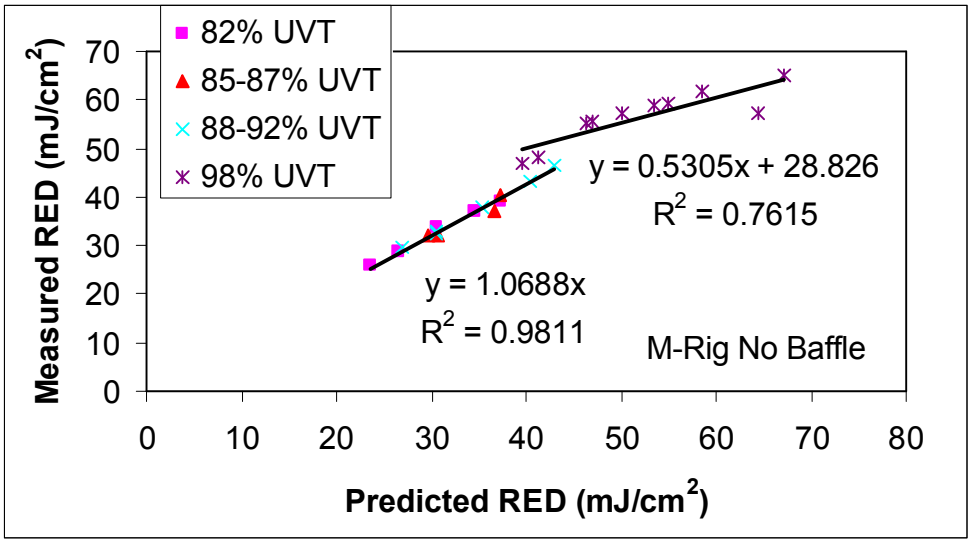

Figure 17. Measured versus predicted B. subtilis RED for the IDI reactor M-rig without baffle plate.

Figure 18 compares the measured B. subtilis RED with the M-rig with baffle plate to the RED predicted using the G1 mesh. Compared to Figure 17, the correlation between measured and predicted RED at lower UVTs is notably less. Furthermore, at low UVTs, the CFD model for the M-rig with the baffle is predicting about 10% higher than with the M-rig without the baffle. The data suggests that the model predictions with the M-rig without the baffle are biased high compared to the prediction with the baffle.

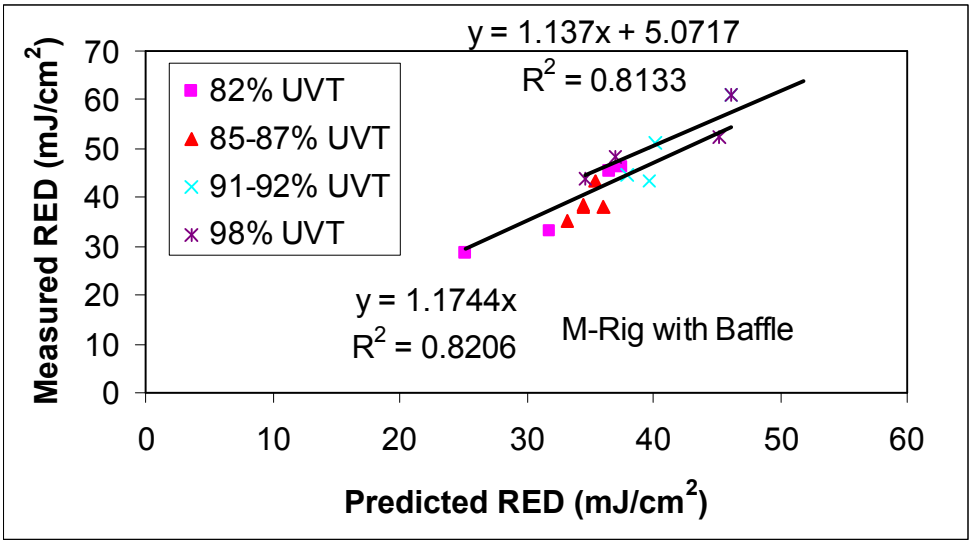

Figure 18. Measured versus predicted B. subtilis RED for the IDI reactor M-rig with baffle plate.

Figure 19 compares the measured B. subtilis RED from the L-rig with baffle plate to the RED predicted using the G1 mesh. Results show that the predicted REDs are consistently lower than the measured REDs by approximately 30% on average.

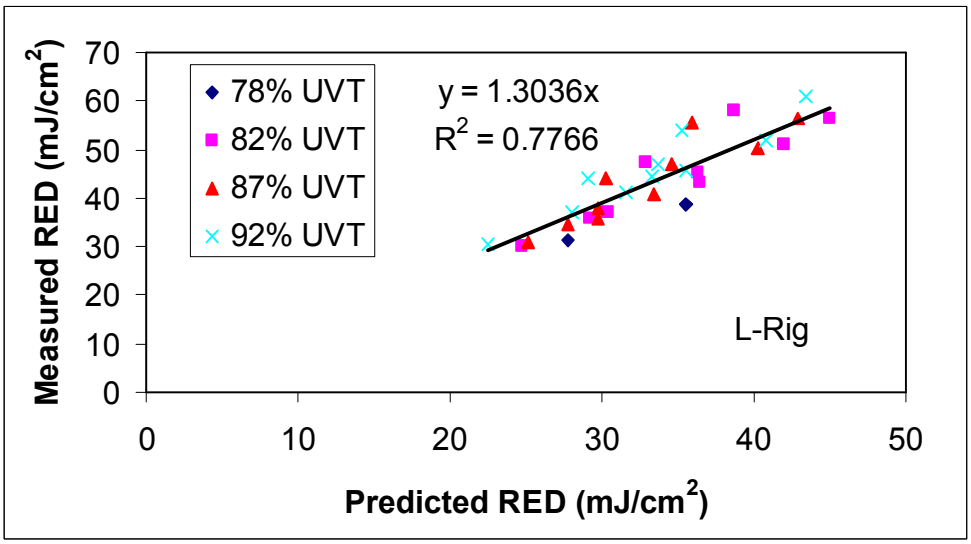

Figure 19. Measured versus predicted B. subtilis RED for the IDI reactor L-rig (one or two reactors without baffle plate).

In contrast to the results obtained with the Calgon reactor, the comparison of the predicted and measured RED with the Ozonia Aquaray® H_2O reactors showed a lower correlation with slopes notably greater than one, even with lower UVTs. Future work will evaluate how model assumptions impact the predicted RED with the objective of resolving these differences. The work will evaluate the assumptions used to model the hydraulics and the particle tracks (e.g. random walk versus no random, starting location), assumptions used with the UV intensity

model (e.g. reflections), and the assumptions used with the inactivation kinetics model (e.g. action spectra).

Summary and Conclusions

Several UV reactor validations have been modeled using numerical techniques to investigate the system hydraulics and dose. The modeling showed that a grid independent solution was developed for each model, both hydraulically and for dose delivery. Modeling showed that at lower UVTs, the models could simulate the measured REDs reasonably well. At higher UVT, wall reflection may become important in the determination of the delivered dose, which is being further evaluated. In general, if these models are shown to reproduce the results of the validation tests, these models can be used a predictive tool for evaluating alternative configurations of inlet or outlet piping to assess the performance of installed systems that differ in configuration from the validated system.

Acknowledgements

This work was funded by AwwaRF project #4107 "*Evaluation of Computational Fluid Dynamics (CFD) as a Cost-Effect Tool for Assessing UV System Performance.*" Sandia is a multiprogram laboratory operated by Sandia Corporation, a Lockheed Martin Company for the United States Department of Energy's National Nuclear Security Administration under contract DE-AC04-94AL85000.

References

Fluent 2006. Fluent 6.3 Users Guide. Lebanon, New Hampshire.

Fluent 2007. Gambit 2.4 User's Guide. Lebanon, New Hampshire.

Ho, C., Khalsa, S., Wicklein, E. and Wright, H. 2008. Important Factors for Computational Modeling of UV Disinfection Systems, 2008 Water Quality Technology Conference, Cincinnati, OH, November 16-20, 2008.

Wright, H. and S. Reddy. 2003. Factors Impacting the CFD-Based Modeling of UV Reactor Performance. AWWA Annual Conference.